NeuroImage 74 (2013) 343–351

Contents lists available at SciVerse ScienceDirect

NeuroImage

journal homepage: www.elsevier.com/locate/ynimg

Characterization of sustained BOLD activation in the rat barrel cortex and neurochemical consequences

Nathalie Just [a,b,*], Lijing Xin [a,b], Hanne Frenkel [a,b], Rolf Gruetter [a,b,c]

[a] Laboratory for Functional and Metabolic Imaging, Ecole Polytechnique Fédérale de Lausanne, Lausanne, Switzerland
[b] Department of Radiology, University of Lausanne, Lausanne, Switzerland
[c] Department of Radiology, University of Geneva, Geneva, Switzerland

ARTICLE INFO

Article history:
Accepted 20 February 2013
Available online 5 March 2013

Keywords:
BOLD
Sustained
Trigeminal
Barrel cortex
Lactate
fMRS

ABSTRACT

To date, only a couple of functional MR spectroscopy (fMRS) studies were conducted in rats. Due to the low temporal resolution of ^{1}H MRS techniques, prolonged stimulation paradigms are necessary for investigating the metabolic outcome in the rat brain during functional challenge. However, sustained activation of cortical areas is usually difficult to obtain due to neural adaptation. Anesthesia, habituation, high variability of the basal state metabolite concentrations as well as low concentrations of the metabolites of interest such as lactate (Lac), glucose (Glc) or γ-aminobutyric acid (GABA) and small expected changes of metabolite concentrations need to be addressed.

In the present study, the rat barrel cortex was reliably and reproducibly activated through sustained trigeminal nerve (TGN) stimulation. In addition, TGN stimulation induced significant positive changes in lactate ($+1.01$ μmol/g, $p < 0.008$) and glutamate ($+0.92$ μmol/g, $p < 0.02$) and significant negative aspartate changes (-0.63 μmol/g, $p < 0.004$) using functional ^{1}H MRS at 9.4 T in agreement with previous changes observed in human fMRS studies. Finally, for the first time, the dynamics of lactate, glucose, aspartate and glutamate concentrations during sustained somatosensory activation in rats using fMRS were assessed. These results allow demonstrating the feasibility of fMRS measurements during prolonged barrel cortex activation in rats.

Introduction

In rodents, the whisker to barrel cortex system is equivalent to the visual system in humans (Petersen, 2007). The whisker sensory system was described more than forty years ago (Woolsey and Van der Loos, 1970) and represents a resourceful model for studying both the structural morphology of the barrel cortex and the function of the whole system. The whiskers of the rodent's snout are arranged in a grid which is replicated in an almost identical manner in layer IV of the primary somatosensory cortex arranged into barrels. Upon deflection of whiskers, action potentials are evoked in the sensory neurons of the infraorbital branch of the trigeminal nerve and information travels to the primary somatosensory cortex (S1) (Petersen, 2007). The whisker to barrel cortex system represents therefore a key model for the investigation of the mechanisms of plasticity (Feldman and Brecht, 2005).

BOLD fMRI investigations in rodents are useful for the understanding and interpretation of the underlying physiological and molecular mechanisms of brain activation. Neurons of the whisker barrel system in the rodent primary somatosensory cortex are known to encode external events in time and space and thus offer an excellent model to study BOLD activation processes (de Celis Alonso et al., 2012; Lu et al., 2003; Yang et al., 1996, 1997). The rat barrel cortex can also be reliably and reproducibly activated through trigeminal nerve (TGN) stimulation (Nielsen and Lauritzen, 2001; Just et al., 2010; Fanselow and Nicolelis, 1999). BOLD responses to short TGN stimulations (30 s) were characterized as a function of stimulus frequency and current intensity (Just et al., 2010) showing robust and reproducible BOLD activation of the primary somatosensory barrel field cortex (S1BF). If sustained stimulation is straightforward in humans (Chen et al., 1993; Prichard et al., 1991; Mangia et al., 2007a,b; Bandettini et al., 1997), it is not as straightforward in rodents due to the difficult control of physiology under anesthesia and adaptation. Prolonged BOLD response in the somatosensory cortex of the rat was first shown in a forepaw rat model (Hyder et al., 1996) where sustained BOLD response lasted 60 min during bilateral forepaw stimulation. Bilateral activation covered the motor and somatosensory areas allowing the delineation of a large voxel for further NMR spectroscopic investigations. Although other groups described a 10-minute BOLD response to forepaw stimulation (Xu et al., 2005), the BOLD response was not characterized.

Numerous studies have been conducted to understand the influence and dynamics of oxygen and glucose supplies to the brain (Mangia et al., 2009). In this context, functional magnetic resonance spectroscopic

* Corresponding author at: Centre d'Imagerie Biomédicale (CIBM), Animal Imaging and Technology Core (AIT), Laboratory for Functional and Metabolic Imaging (LIFMET), Centre d'Imagerie Biomédicale (CIBM), CH-1015 Lausanne, Switzerland. Fax: +41 21 6937960.
E-mail address: nathalie.just@epfl.ch (N. Just).

1053-8119/$ – see front matter © 2013 Elsevier Inc. All rights reserved.
http://dx.doi.org/10.1016/j.neuroimage.2013.02.042

(fMRS) techniques have been developed and improved to complement previous investigations and our understanding of the role of metabolites during brain activation (Chen et al., 1993; Prichard et al., 1991; Mangia et al., 2007a,b). In-vivo ^{1}H fMRS allows the non-invasive measurement of brain metabolites during brain activation. To date, successful fMRS studies were conducted at high magnetic field strength (7 T) in the human visual cortex (Mangia et al., 2007a,b). These studies demonstrated that sustained neuronal activation raises oxidative metabolism to a new steady-state and supports the astrocyte-neuron lactate shuttle (ANLS) hypothesis with an increase in lactate and a decrease in glucose levels during visual cortex activation. In rodents, fMRS studies suffer from lower signal to noise ratio due to smaller voxels of interest. In addition, due to the mismatch in temporal resolution between BOLD fMRI using echo planar imaging (2 s) and current proton MRS techniques (2–3 min), increased brain activation durations with little habituation processes under light anesthesia are requested.

For an accurate understanding of the link between metabolic and functional mechanisms in the brain, it is essential to develop BOLD fMRI and fMRS methodologies in conjunction with appropriate functional paradigms. The goal of the present study was to characterize the BOLD response in the barrel cortex of the rat during continuous trigeminal nerve stimulation and demonstrate the feasibility of fMRS measurements during prolonged barrel cortex activation.

Materials and methods

Animal preparation

All animal procedures were performed according to the federal guidelines of the Animal Care and approved by the local authority. Male adult Sprague–Dawley rats (n = 11, 350 ± 40 g) were initially anesthetized with isoflurane in a mixture of O_2. Each rat was orally intubated. A femoral artery and a femoral vein were catheterized for α-chloralose administration and blood gas sampling. After fixing the rat head using ear and bite bars, the rat was positioned in a dedicated holder. The breathing rate was monitored simultaneously with body temperature throughout the experiment with a rectal probe (Model 1025, SA Instruments Inc. Stony Brook, NY, USA). Body temperature was maintained at 37.5 °C ± 0.5 °C with temperature-controlled circulating water placed under the rat. The blood pressure was monitored through a transducer attached to the catheterized femoral artery (SA Instruments Inc. Stony Brook, NY, USA).

After surgery, anesthesia was switched from isoflurane to α-chloralose; an initial intravenous dose of 80 mg/kg was administered followed by a continuous intravenous infusion of 27 mg/kg/h at a rate of 2 ml/h.

Blood gases were sampled every 30 min for the first 90 min and then every hour until the end of the full experiment (between 5 and 8 h after the start) and blood parameters were maintained at physiological levels (see Table 1) throughout the experiment.

During trigeminal nerve stimulation, no blood sampling was performed to maintain the rat physiology under normal conditions. However, respiration, temperature and blood pressure were carefully and continuously controlled during the entire course of prolonged stimulation. In 4 rats, pH, pCO_2 and pO_2 were controlled before, during and after prolonged TGN stimulation.

Trigeminal nerve stimulation

Two stainless steel electrodes were percutaneously inserted either in the left or right trigeminal nerve. The cathode was inserted in the hiatus infraorbitalis as described in Nielsen and Lauritzen (2001) and the anode was inserted in the masticatory muscles. Electrical stimulation of one trigeminal nerve was performed by delivering square pulses using an external stimulator (WPI, Stevenage, UK) (Just et al., 2010). Previous investigations using TGN electrical stimulations demonstrated that the BOLD response was optimized for stimulation currents in the range 1–3 mA and for a stimulation frequency of 1 Hz (Just et al., 2010). Experiments were performed with a current intensity of 2 mA and a stimulation frequency of 1 Hz. The duration of a stimulation pulse was 0.3 ms.

fMRI protocol

All the experiments were performed on an actively shielded 9.4 T/31 cm horizontal bore magnet (Magnex, Varian, Abingdon, UK) with 12 cm gradients (400 mT/m in 120 μs) with a quadrature transmit/receive 17 mm surface coil. First and second order shims were adjusted using FAST(EST)MAP (Gruetter and Tkác, 2000) resulting in water linewidth of 13–15 Hz in a 216 μl ($6 \times 8 \times 4.5$ mm^3) volume. The BOLD response was assessed using single shot gradient echo EPI (TR/TE = 2500–2000/25 ms; FOV = 20 × 20 mm; matrix = 64 × 64; slice thickness = 0.5–1 mm; 5–6 slices, bandwidth = 325 kHz, 300–960 volumes). The echo re-alignment was performed using a reference scan (Lei et al., 2008).

Data analysis

Post-processed images were analyzed with SPM8 (MATLAB; The MathWorks; Natick, USA; Statistical Parametric Mapping, www.fil.ion.ucl.ac.uk/spm/) using the general linear model (GLM) analyzing each voxel independently and creating a parametric map of statistical significance (Friston et al., 1995). Within each analysis, the mean global intensities were mean scaled to an arbitrary value. Gradient echo (GRE-EPI) time series were realigned and spatially smoothed with a 3D Gaussian kernel. The design model tested was a comparison between 'off' and 'on' conditions within each TGN stimulation paradigm. The paradigm was convolved with SPM's hemodynamic response function defined as a gamma-variate function and high pass-filtered (128 s for a 1 min OFF–30 s ON–1 min OFF paradigm, >400 s for a 2 min OFF–10 min ON–2 min OFF paradigm of stimulation). Residuals for the realigned rat movement were taken into account by submitting the realignment

Table 1
Physiological parameter measurements taken at different time points during α-chloralose anesthesia and during fMRI sessions (mean ± S.D).

Time	pH	pCO_2 (mm Hg)	pO_2 (mm Hg)	T (°C)	MABP (mm Hg)	HR
0 min	7.39 ± 0.04	43.0 ± 6.9	245 ± 97	37.4 ± 0.4	153 ± 10	400 ± 5
30 min	7.4 ± 0.03	42.5 ± 4.8	275.0 ± 67	37.5 ± 0.8	133 ± 15	395 ± 7
60 min	7.4 ± 0.04	41.2 ± 4.3	278.8 ± 58	37.5 ± 0.8	137 ± 12	391 ± 7
90 min	7.35 ± 0.07	39.7 ± 6.5	280.8 ± 76	37.7 ± 0.5	138 ± 11	385 ± 5
150 min	7.37 ± 0.04	37.95 ± 4.8	334.0 ± 57.6	37.5 ± 0.1	150 ± 12	390 ± 5
210 min	7.39 ± 0.06	38.4 ± 8.6	349.7 ± 144.9	38.0 ± 0.7	160 ± 20	385 ± 5
270 min	7.39 ± 0.04	41.95 ± 11.36	375.3 ± 144.5	37.6 ± 0.3	166 ± 18	395 ± 7
310 min	7.38 ± 0.04	37.32 ± 9.0	323.8 ± 136.7	37.3 ± 0.6	152 ± 15	392 ± 7
370 min	7.43 ± 0.06	36.27 ± 7.77	281.2 ± 70.5	37.6 ± 0.3	155 ± 15	385 ± 5
480 min	7.4 ± 0.04	34.7 ± 4.2	330.4 ± 114	37.4 ± 0.5	145 ± 10	381 ± 5
Mean	7.4 ± 0.05	39.7 ± 7.0	280.0 ± 95.0	37.6 ± 0.6	148.9 ± 10.6	389.9 ± 6

parameters (translations and rotations) as regressors. T-maps were calculated on a pixel by pixel basis. Thresholding criteria of 5 adjacent voxels, each with a T score > 3.0 were used to identify regions of interest. Only clusters comprising at least 5 pixels were considered significant ($p < 0.0001$ (uncorrected)).

With STIMULATE (University of Minnesota, Minneapolis, USA) (Strupp, 1996), regions of interest (ROIs) over the activated primary somatosensory barrel field cortex (S1BF) were drawn with respect to the Paxinos and Watson's atlas (Paxinos and Watson, 1998). ROIs were delineated from the thresholded T-map of each rat. A representative average time-course was recorded for each animal. When needed baseline correction was performed. T-maps were overlaid on single shot gradient echo EPI images.

STIMULATE was also used for constructing BOLD T-maps as a function of time during stimulation. 10-minute BOLD time courses during TGN stimulation were divided into four shorter periods: 2–2.4 min, 2–4 min, 4–8 min and 8–12 min. Each period was statistically compared to the rest periods to create parametric T-maps.

Data were presented as means ± SEM or S.D.

fMRS

Localized proton spectroscopy was performed using Spin Echo Full Intensity Acquired Localized Sequence (SPECIAL) (Mlynárik et al., 2006) (TR/TE = 4000/2.8 ms; BW = 5000 Hz) in a VOI localized in the activated barrel cortex and after adjusting once more the shims using FASTMAP. The unsuppressed water signal was measured at the end of the experiment. The voxel size for ^{1}H MRS was $2 \times 2 \times 4$ mm^3 and was positioned on the BOLD activation maps (motion-corrected T-value maps (GLM model) with $t > 3$) obtained after a 10-minute TGN stimulation. When distortions were found at 1.3 ppm in the lactate region, data were entirely discarded from the study.

The raw ^{1}H MRS spectra were corrected for frequency drift and then summed for LCModel analysis (Provencher, 1993) with a basis set of 21 stimulated metabolites and measured macromolecular baseline.

The signal to noise ratio (SNR) of a spectrum was calculated by measuring the intensity of the largest peak in the spectral range, N-acetylaspartate in this instance, and then measuring the noise intensity in the spectral range 0.0–0.5 ppm.

Metabolite time courses

For metabolite concentration time courses, blocks of 16 fids were summed using a moving average (3×16 fids ~ 1 min, $SNR_{LCModel} > 8$; full width at half maximum < 0.040 ppm) over each 10-minute period per rat and then further summed over all the animals.

Statistical analysis

Statistics were performed using a paired t-test. A p value < 0.05 was considered significant. In some cases a p value of 0.07 was also taken into consideration to indicate that comparisons were approaching significance.

Results

Physiological measurements and sustained trigeminal nerve stimulation

The physiological measurements (pH, pCO_2, pO_2 and temperature) during the entire course of the experiments are reported in Table 1. In Table 2, pH, PO_2, PCO_2, heart rate (HR) and mean arterial blood pressure (MABP) are reported for measurements performed half an hour before 10-minute TGN stimulation, at 5 min during stimulation and half an hour after TGN stimulation for 4 rats showing no significant changes ($p > 0.05$, t-test).

Typical examples of BOLD time-courses are shown (Fig. 1) during direct trigeminal nerve stimulation (S1BF, primary somatosensory barrel field cortex). The stimulation time was progressively extended: stimulation durations were 30 s, 1 min (Fig. 1.D), 5 min, 10 min (Fig. 1.E) and 25 min while gradient echo EPI acquisitions were performed for 30 min. A unilateral cluster of active pixels was well-delineated within the barrel cortex during prolonged TGN stimulation for 11 rats (Figs. 1B and C).

Comparison of short versus long activation of the barrel cortex

Short TGN stimulation (30 s ON–1 min OFF–30 s ON–1 min OFF) or (60 s ON–60 s OFF–60 s ON–60 s OFF) and sustained TGN stimulation (2 min OFF–10 min ON–2 min OFF) were compared to assess potential the temporal and spatial changes in the activation of the rat barrel cortex. T-maps overlaid on single shot gradient echo EPI images for each paradigm demonstrate that unilateral BOLD activation extends over S1BF during short and sustained stimulations. T-value maps obtained during a short stimulation paradigm (Fig. 1.B) as depicted by the corresponding barrel cortex BOLD time course (Fig. 1D) demonstrated strong BOLD activation in S1BF. Upon onset of long TGN stimulation, an initial BOLD peak was found followed by a BOLD response that plateaus before returning to baseline (Fig. 1E). Individual sustained BOLD responses typically demonstrated a characteristic overshoot at onset of stimulation as well as a characteristic post-stimulus BOLD undershoot lasting a few seconds. The area of activation was not significantly decreased during sustained stimulation although a tendency to a decreased number of active pixels was seen. The mean BOLD response across rats for both paradigms showed no significant difference between short (% change = 2.2 ± 0.5%) and long stimulations (% change = 2.7 ± 1%).

Evaluation of BOLD effect as a function of time during prolonged stimulation

BOLD activation was present in the barrel cortex until the end of the stimulation: 10-minute BOLD stimulation time courses were divided into shorter time periods. Each period was compared to the 2-minute pre- and post-stimulus baselines using t-tests for statistical analysis (Fig. 2.B). T-maps were constructed from these comparisons (Fig. 2.A). The number of active pixels within the barrel cortex was highest for T-maps obtained during the first 2 min of the long TGN stimulation and progressively decreased during TGN stimulation. The number of active pixels within the barrel cortex was significantly decreased during the last 4 min of TGN stimulation (t-test, $p < 0.006$) (Fig. 2.C) but remained localized in the area of interest (Fig. 2.A). Upon onset of

Table 2
Physiological parameters measured before, during and after TGN stimulation in 4 rats (mean ± S.D).

	pH	pCO_2 (mm Hg)	PO_2 (mm Hg)	T (°C)	HR	MABP (mm Hg)
Before stimulation	7.33 ± 0.02	39.7 ± 4.3	248 ± 80	37.5 ± 0.5	365 ± 10	153.25 ± 9
At 5 min during stimulation	7.30 ± 0.1	40 ± 6.9	252 ± 58	37.5 ± 0.5	370 ± 15	157.5 ± 7.6
After stimulation	7.33 ± 0.03	38.5 ± 5.2	259 ± 73	37.5 ± 0.5	373 ± 13.5	159 ± 9

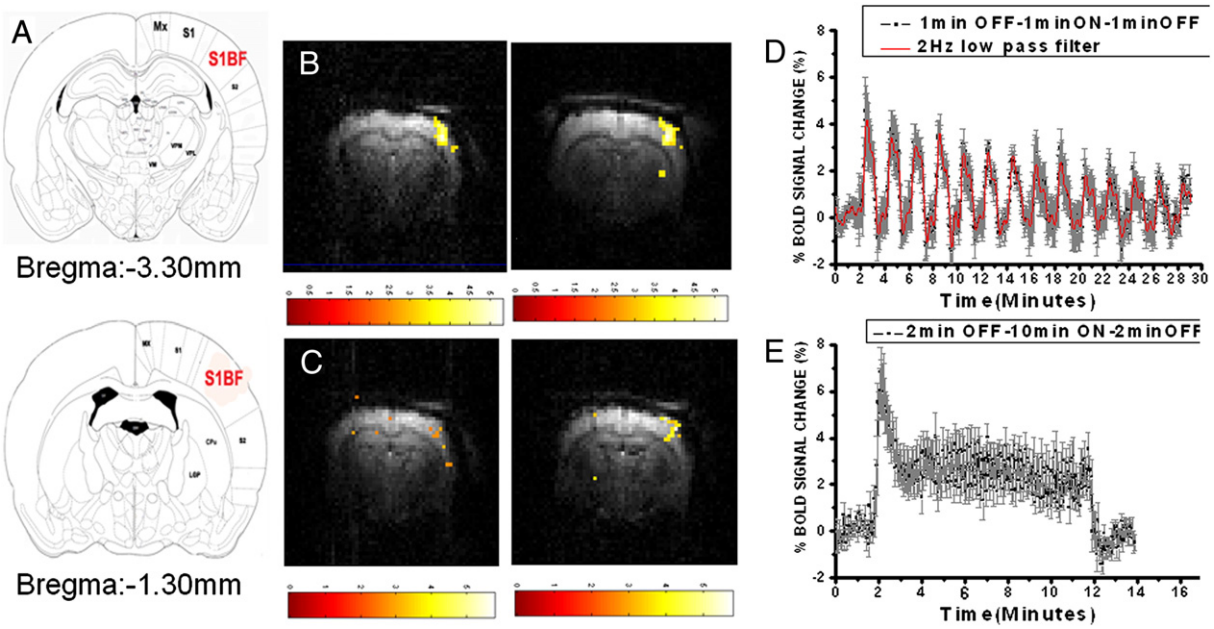

Fig. 1. Examples of BOLD mapping in the barrel cortex following sustained trigeminal nerve stimulation. T-maps overlaid on single shot gradient echo EPI images for short and sustained paradigms demonstrate that unilateral BOLD activation is located in S1BF and during short and trigeminal nerve sustained stimulation. A. Accurate positioning of the slices was done on fast-spin echo images (Fig. 1; Suppl file) and according to the Paxinos and Watson's atlas between 0 and −4 mm distance to the bregma. B. T-map of the BOLD activation of the barrel cortex following a 1 min OFF–1 min ON–1 min OFF TGN stimulation repeated up to 30 min. C. T-map of the BOLD activation of the barrel cortex following a 2 min OFF–10 min ON–2 min OFF TGN stimulation. D. 1 min OFF–1 min ON–1 min OFF BOLD time course E. Mean 10 min BOLD time course (n = 11) for a 2 min OFF–10 min ON–2 min OFF paradigm of stimulation (mean ± SEM).

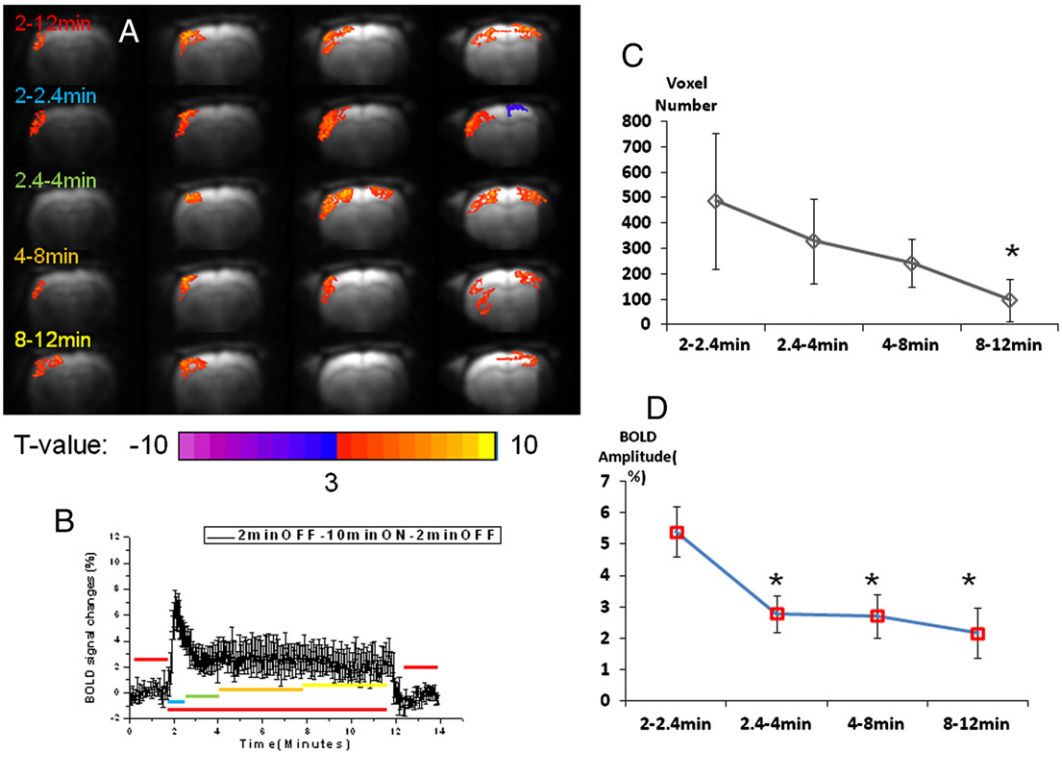

Fig. 2. Stimulation time-dependent fMRI results. The 10-minute stimulation period was divided into four stimulation periods to compare with baseline: 2–2.4 min, 2.4–4 min, 4–8 min, and 8–12 min. The number of activated pixels with a t-value > 3 in the barrel cortex was determined. A. T-value maps overlaid over single shot gradient-echo EPI images are shown for the baseline vs 2–12 min stimulation period (red code), for the baseline vs. 2–2.4 min stimulation period (blue code), for the baseline vs. 2.4–4 min stimulation period (green code), for the baseline vs. 4–8 min stimulation period (orange code), and for the baseline vs. 8–12 min stimulation period (yellow code). B. Mean 10-minute BOLD (±SEM) response in the rat barrel cortex averaged across 11 rats. Color codes were given to indicate the times given to obtain T-maps during sustained TGN stimulation. C. The area of stimulation within the barrel cortex decreased as a function of time. The last 4 min of TGN stimulation showed significantly less active pixels in the rat barrel cortex ($p < 0.006$).D. Upon onset of TGN stimulation, the BOLD response rose up to 5.4 ± 0.8% before decreasing significantly during the remaining stimulation time (t-test, $p < 0.0001$). During the remaining 9 min of TGN stimulation, BOLD responses remained constant.

TGN stimulation, the BOLD response rose up to 5.4 ± 0.8% before decreasing significantly during the remaining stimulation time (t-test, $p < 0.0001$). During the remaining 9 min of TGN stimulation, BOLD responses remained constant (Fig. 2D).

Blood oxygen level dependent changes in the barrel cortex and voxel localization

With sustained trigeminal nerve stimulation, BOLD activation within the barrel cortex was robust and reproducible for a period time of 10 min with little habituation processes. The location and size of the voxel of interest ($2 \times 2 \times 4$ mm^3) (Fig. 3.A) was carefully chosen to avoid lipid contamination and permit enough SNR. Shimming within the barrel cortex resulted in water linewidths between 12 and 15 Hz. To evaluate whether TGN stimulation was effective or not, the total creatine peak height was measured during rest and stimulation periods (Fig. 3B). The BOLD effect induced an increase of T_2^* within the barrel cortex that translated into a decrease of the NAA and tCr linewidth and an increased peak height of up to 3.5%. The position of the voxel of interest for further fMRS was based on the detection of a positive difference on the total creatine height with respect to the BOLD T value maps. Figs. 3.C and D present examples of raw proton spectra acquired during 10-minute TGN stimulation and 10-minute rest respectively for an SNR of 93 and 83 respectively. The corresponding LCModel fits and residuals to each of these spectra with no lipid contamination in the 1.3 ppm region are also presented in Figs. 3.D and E.

Quantitative analysis of metabolites during 10-minute TGN stimulation

The signal to noise ratio of N-acetylaspartate in single scan spectra (16 blocks) was typically between 16 and 26.The signal to noise ratio value of NAA for a spectrum of 160 scans was 83 and 93 respectively (Figs. 3C, D). On average, the mean signal to noise ratio was 52.6 ± 5.6 (SEM). Using LCModel, 16 metabolites were reliably quantified. Metabolites of interest such as lactate and aspartate had Cramer–Rao lower bounds (CRLB) under 35% while glutamate and glutamine had CRLB under 8%. For Glc, quantification was considered reliable in the present study for CRLB under 40%. The neurochemical profiles for 16 metabolites as well as the PCr/Cr ratio were compared during the first 10 min of rest, the first 10 min of stimulation and the first 10 min of recovery (Fig. 4). Changes for metabolites of interest are summarized in Table 3 with their significance level. Lactate was significantly higher compared to both recovery and rest periods ($p < 0.008$) while glutamate was only significantly higher with respect to the recovery period ($p < 0.02$) but the difference in Glu levels approached significance with respect to the rest period ($p \sim 0.07$). In a similar way aspartate levels were significantly smaller with respect to the rest period ($p < 0.004$) and only approached significance with respect to the recovery period ($p \sim 0.07$). Glucose levels decreased by 9.5% and 16% with respect to the rest and recovery periods but did not reach significance levels. Glutamine, γ-aminobutyric acid (GABA) and the ratio PCr/Cr only slightly decreased during TGN stimulation with respect to the first rest period without reaching statistically significant levels.

Quantification of metabolite changes using a difference spectrum

A 0.8 Hz line broadening of the tCr peak was applied to the stimulation spectrum (Fig. 5A) in order to match the linewidth of the rest spectrum (Fig. 5B).

The difference spectrum ($n = 11$) before (Fig. 5.C) and after correction (Figs. 5D and E) is shown.

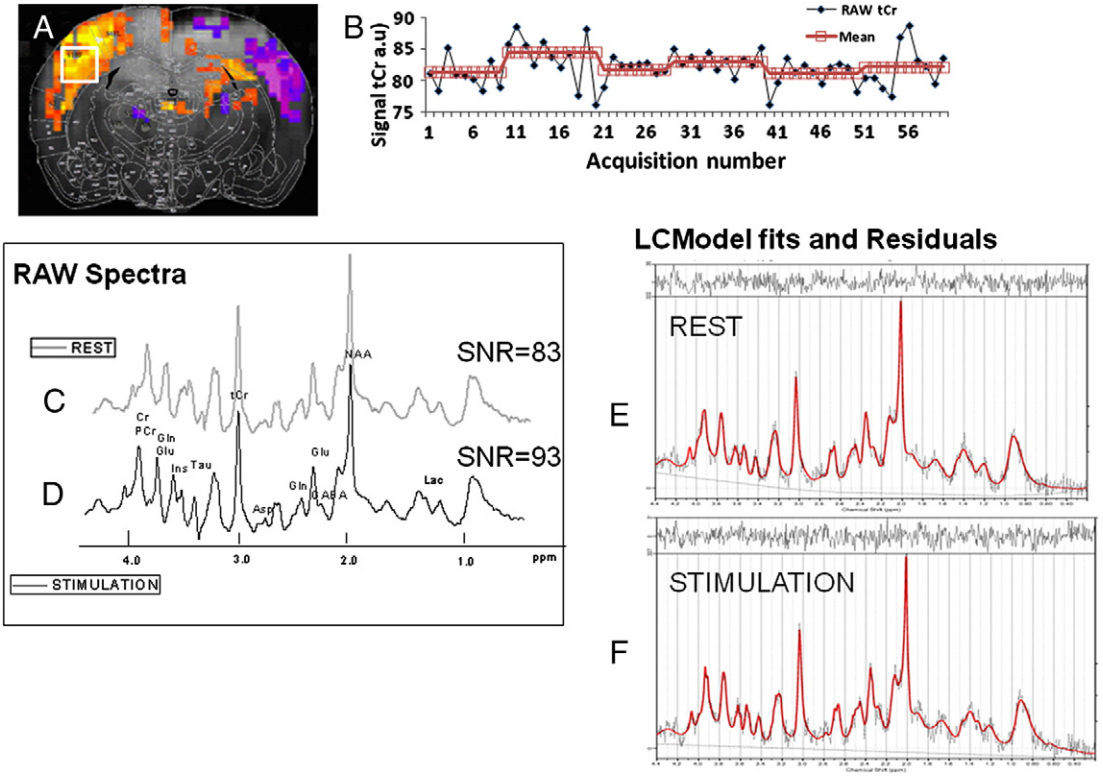

Fig. 3. Localization of the voxel of interest for fMRS and quality of proton spectra. A. Gradient echo EPI image with overlaid T-value map and Paxinos' atlas showing strong activation in the rat barrel cortex and the localized $2 \times 2 \times 4$ mm^3 voxel of interest. B. Example of total creatine signal time course during 10 min OFF–10 min ON–10 min OFF–10 min ON paradigm of activation showing a 3.5% increase of the signal height during TGN stimulation due to the BOLD effect. C, D. Examples of labeled raw proton spectra acquired during 10-minute TGN stimulation (STIMULATION) and 10-minute rest (REST) respectively for an SNR of 93 and 83 respectively. NAA: N-acetylaspartate; Glu: glutamate, GABA: γ-aminobutyric acid; Glc: glucose, tCr: total creatine; PCr: phosphocreatine; Asp: aspartate; Gln: glutamine; Lac: lactate. E, F. LCModel fits and residuals to each of these spectra are also presented.

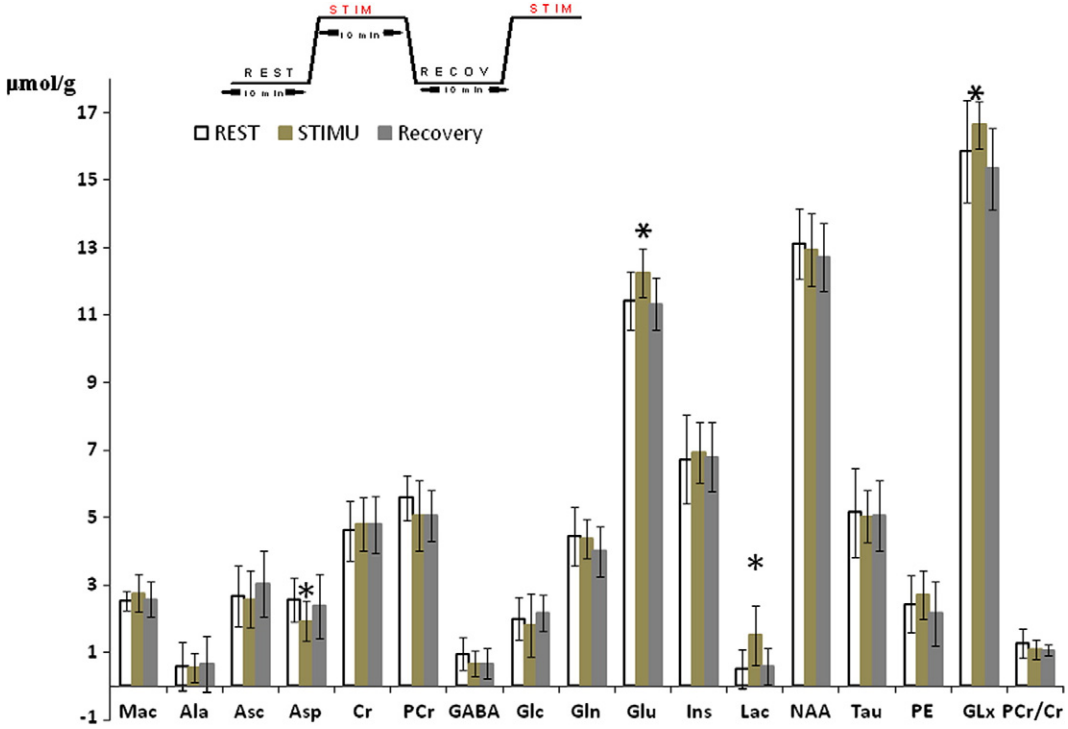

Fig. 4. LCModel quantification of 16 metabolites for the first 10-minute rest period, the first 10-minute TGN stimulation and the first 10-minute recovery period for 11 rats. * indicates significance level $p < 0.05$.

The BOLD-free difference spectrum (Fig. 5E) demonstrated positive peaks for lactate (Lac: 1.32 ppm) and glutamate (Glu: 2.15, 2.36 ppm) as well as negative peaks for aspartate (Asp: 2.6 and 2.8 ppm) and glucose (Glc). These peaks represent the relative resulting changes in metabolite concentration due to TGN stimulation. Figs. 5F and G represent the difference of the LCModel fits to the stimulation spectrum (Fig. 6A) and the rest spectrum (Fig. 5B) and the residuals. From these fitting procedures metabolic differences were calculated: Asp = 0.63 ± 0.4 µmol/g representing 19% change, Glu = 0.9 ± 0.2 µmol/g representing 8.5% change, and Lac = 0.26 ± 0.12 µmol/g representing 70% change. Glc was not fitted.

Time course of metabolites

Fig. 6.A depicts the methodology that was used to obtain metabolite time courses in the rat barrel cortex during 10-minute TGN and stimulation periods. The time courses for 11 rats of Lac (CRLB ~ <30%), Glu (CRLB ~ <5%), Glc (CRLB ~ <40%) and Asp (CRLB ~ <30%) are depicted in (Figs. 6.B–E) for a 10-minute TGN stimulation period and a 10-minute rest period. These time courses reveal that Lac increased steeply upon onset of TGN stimulation (+0.5 ± 0.14 µmol/g) and kept at steady state levels (0.95 ± 0.08 µmol/g) until the end of stimulation where Lac levels decreased progressively towards basal levels (0.48 ± 0.06 µmol/g). During the stimulation the Lac rate of change was 0.07 µmol/g/min at steady state approximately. Simultaneously, glutamate kept at higher levels during stimulation (12.14 ± 0.2 µmol/g versus 11.47 ± 0.09 µmol/g) at a rate ranging between 0.12 and 0.33 µmol/g/min during stimulation while glucose continuously decreased (mean rate of decrease: 0.145 ± 0.06 µmol/g/min) before increasing again during the recovery period. Aspartate also demonstrated a tendency to decrease (mean rate of decrease: 0.113 ± 0.07 µmol/g/min) upon onset of stimulation towards mid-stimulation time (~5 min).

Discussion

In rodents, the development of a robust and reproducible model for sustained stimulation is mandatory for further investigations using either ^{1}H or ^{13}C functional NMR spectroscopic measurements (Xu et al., 2005; Yang and Shen, 2006). The trigeminal nerve stimulation model

Table 3
Absolute concentration of metabolites and their changes with respect to the rest period prior to the first 10-minute TGN stimulation and the recovery period after the first 10-minute TGN stimulation (*p < 0.05; +p = 0.07).

Metabolite	Rest	Stimulation	Recovery	Stimulation–rest		Stimulation–recovery	
	Concentration ± S.D			Change ± S.D	Change (%)	Change ± S.D	Change (%)
	(µmol/g)			(µmol/g)		(µmol/g)	
Ala	0.59 ± 0.7	0.55 ± 0.42	0.67 ± 0.83	−0.04 ± 0.73	−6.8%	−0.12 ± 0.71	−18%
Asp	***2.57 ± 0.65***	***1.94 ± 0.59*↓**	***2.38 ± 0.96***	***−0.63 ± 0.60****	***−24%***	***−0.44 ± 0.58 †***	***−18.5%***
GABA	0.96 ± 0.49	0.68 ± 0.38	0.68 ± 0.44	−0.28 ± 0.42	−29%	0.0003 ± 0.62	0%
Glc	2.01 ± 0.63	1.82 ± 0.93	2.16 ± 0.54	−0.19 ± 1.29	−9.5%	−0.35 ± 1.00	−16.2%
Gln	4.44 ± 0.86	4.37 ± 0.56	4.0 ± 0.75	−0.07 ± 0.49	−1.6%	0.37 ± 0.56	+9.25%
Glu	***11.41 ± 0.87***	***12.26 ± 0.71*** ↑	***11.34 ± 0.77***	***0.85 ± 1.01*** †	***+7.5%***	***0.92 ± 0.88****	***+8%***
Lac	***0.51 ± 0.58***	***1.51 ± 0.89*** ↑	***0.60 ± 0.53***	***1.01 ± 0.57****	***+198%***	***0.91 ± 0.87****	***+152%***
Glx	15.85 ± 1.50	16.63 ± 0.71	15.54 ± 1.20	0.78 ± 1.38	+4.9%	1.29 ± 1.09*	+8.3%
PCr/Cr	1.28 ± 0.42	1.08 ± 0.29	1.07 ± 0.17	−0.2 ± 0.37	−11%	0.01 ± 0.31	+0.9%

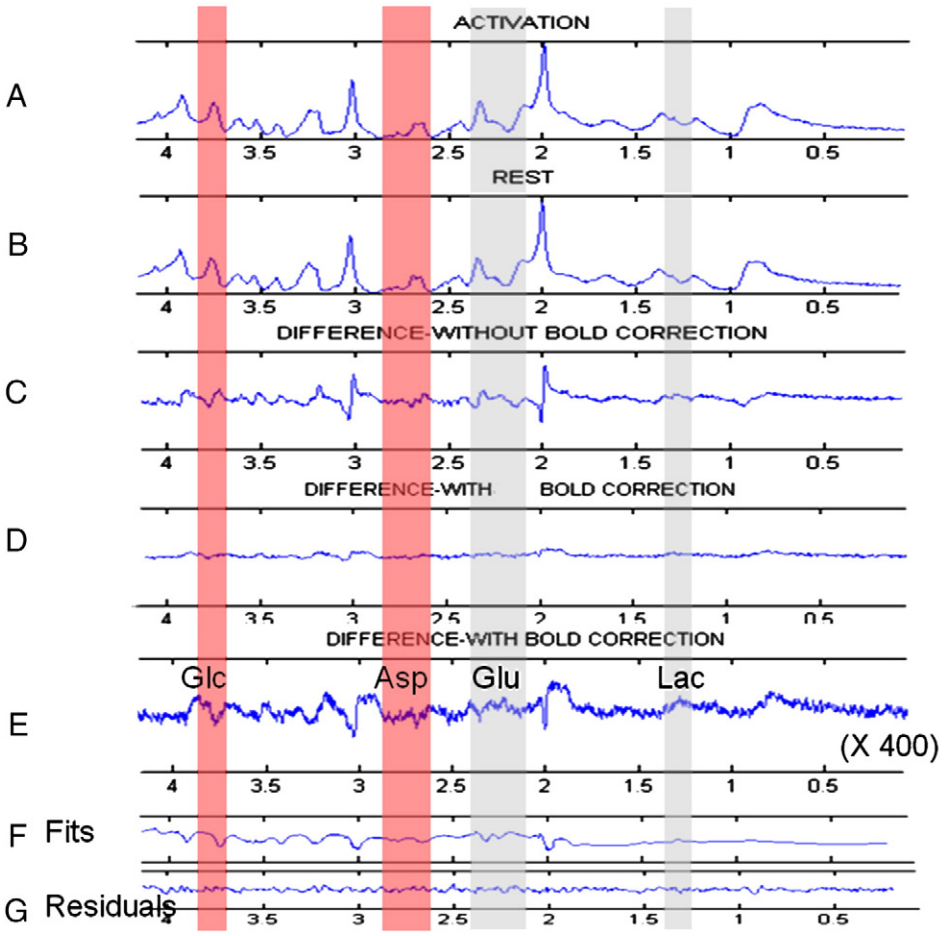

Fig. 5. Correction for T2* effect and BOLD free difference spectrum. A. Summed stimulation spectra (n = 11). B. Summed rest spectra (n = 11). C. Difference spectrum between A and B before line-broadening of the group stimulation spectrum. D, E. BOLD free difference spectrum after applying a 0.8 Hz line-broadening to the group stimulation spectrum showing positive lactate (1.32 ppm) and Glu peaks (2.15 ppm) and negative Asp (2.6 and 2.8 ppm) and Glc peaks. A 0.8 Hz line broadening (lb) of the tCr peak was applied to the stimulation spectrum in order to match the linewidth of the rest spectrum. F, G. Difference of LCModel fits to spectra A and B and residuals. Shaded gray lines indicate positive Lac and Glu peaks. Shaded red lines indicate negative peaks.

induced robust and intense BOLD activation in the barrel cortex for a well-defined range of stimulus current intensities and stimulus frequencies using a short stimulation paradigm (Just et al., 2010). Prolonged TGN stimulation demonstrated that BOLD activation takes place similarly in the primary somatosensory barrel field cortex although the number of active pixels was only slightly decreased compared to short stimulation.

Usually, habituation can be observed as a decline of the BOLD response as a function of time during the stimulation period and represents a decrease in neuronal firing. During sustained TGN stimulation, the stimulus amplitude, frequency and duration were kept below the threshold of nociception where the stimulation induces systematic mean arterial blood pressure increases indicating painful stimulation. Strong adaptation was rarely observed for 10 min of TGN stimulation at a stimulus frequency of 1 Hz and under normal physiological conditions. A few measurements during 10-minute TGN stimulation periods demonstrated that blood pressure, heart rate and PCO_2 showed no statistically significant changes. The level of adaptation during barrel cortex activation demonstrated to be frequency-dependent with adaptation becoming significantly stronger at 2 Hz and above (Chung et al., 2002). Yet, a BOLD signal overshoot at the beginning of stimulation followed by an equilibration to a new steady state, as was the case in the present study, was usually interpreted as an adaptation phenomenon (Uludağ, 2008). The significant decrease of the number of active voxels towards the end of TGN stimulation and the significant change in BOLD amplitude during the first few seconds of stimulation may confirm this. Nevertheless, the present study also confirmed that BOLD activation of the barrel cortex was present until the end of stimulation and that the BOLD effect remained at stable amplitude during the last 9 min of stimulation.

Sustained BOLD activation in the barrel cortex of the rat was present in the same areas (S1BF and S2) than during short BOLD activation (Just et al., 2010). Quantitatively, the relative BOLD signal change was not significantly different during sustained TGN stimulation than during short TGN stimulation. Prolonged whisker stimulation modulates the magnitude of the responses generated by thalamo-cortical afferents of the stimulated pathway leading to a decreased activation within the barrel cortex (Quairiaux et al., 2007). These effects could explain the progressive decreased number of active pixels seen during a 10-minute TGN stimulation period.

Functional magnetic resonance spectroscopy during sustained trigeminal stimulation

The robust and reproducible BOLD activation of the barrel cortex during sustained TGN stimulation allowed positioning accurately the VOI for further metabolic investigations. When significant distortions of ^{1}H NMR spectra were seen due to external lipid contamination occasioned by the proximity of the barrel cortex to the skull or motion, spectra were discarded from the study (see Supplementary file).

The summation of 10-minute rest spectra and 10-minute stimulated spectra followed by the quantification of metabolites using LCModel allowed to determine significant lactate (+198%) and glutamate (+7.5–8%) increases during barrel cortex activation and significantly

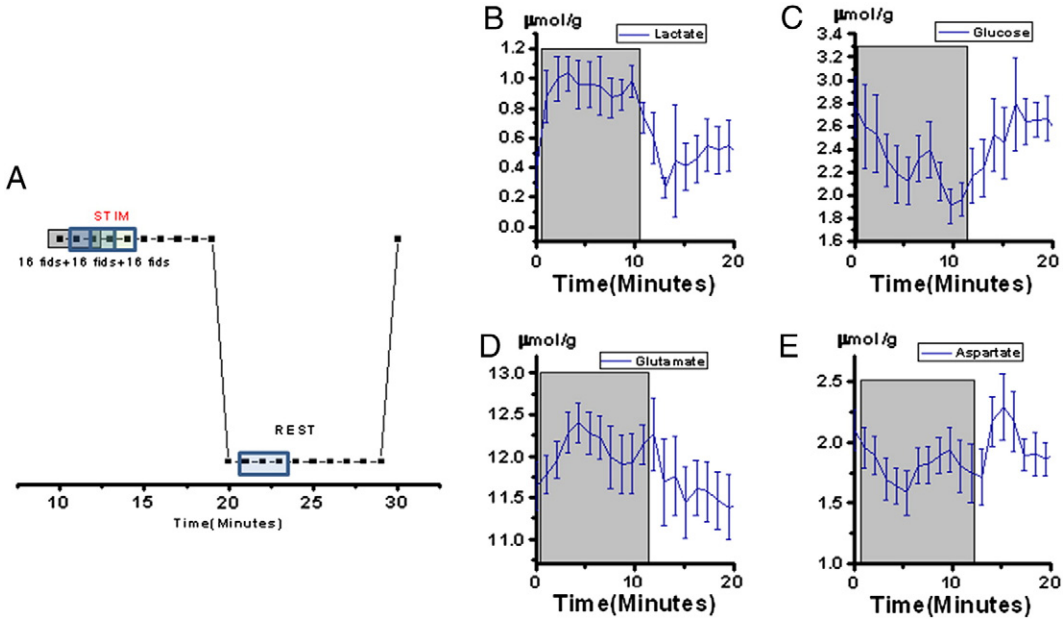

Fig. 6. Lactate, glucose, aspartate and glutamate time courses. A. Each acquisition represented 16 fids for a temporal resolution of 1 min. Three consecutive points were summed as a function of time representing 48 fids and allowing increasing the SNR per point while the temporal resolution was preserved. Shaded boxes indicate the points taken into account for calculation of the moving average. This procedure was applied to the first stimulation and first recovery period and averaged across rats. B, C, D, E. Metabolite time courses in µmol/g for lactate, glucose, glutamate and aspartate. Data are mean ± SEM. The shaded areas show the periods of TGN stimulations.

decreased levels of Asp (−24%) among several other metabolites. These changes were confirmed by the changes as function of time observed during TGN stimulation (Fig. 6). However, the quantitative analysis did not show significant Glc changes although the trends in Glc time courses were obvious. We attributed this result to variability of Glc concentrations between subjects.

These results were in good agreement with the direction of concentration changes observed by Mangia et al. (2007a,b) during human visual stimulation (Glu = +3%; Asp −15%; Lac = +20%). In addition, these results were supported by the BOLD free difference spectrum (Fig. 5) demonstrating positive Lac and Glu peaks as well as negative Asp and Glc peaks during successive 10-minute TGN stimulation periods. Fitting the difference spectrum in order to quantify the changes in metabolite concentrations induced during the barrel cortex activation is expected to give a more robust quantitative analysis of the changes induced during sustained barrel cortex activation.

Compared to fMRS acquisitions performed at 7 T in a human scanner using the exact same MR spectroscopic technique and taking into account differences in voxel sizes, number of averages and B0 field, the SNR of a single proton spectrum was 1.5 times lower (VOIsize = $20 \times 22 \times 22$ mm^3, 2 scans at 7 T versus VOIsize = $2 \times 2 \times 4$ mm^3, 160 scans at 9.4 T) and a large variability of SNR was detected across rats that we attribute to changes in our surface coil performances as well as changes in shimming quality during acquisition. Although, the physiology was carefully controlled during each experimental session as shown in Table 1, we avoided blood sampling during stimulation periods and performed bench tests on 4 animals only showing no effects during TGN stimulation. However, within the magnet, we cannot completely discard potential changes in physiology during proton spectroscopic acquisitions coupled with TGN stimulations. Therefore, the noise contribution in the BOLD free difference spectrum remained important and prevented using the LCModel to quantify changes in metabolites during stimulation. Current developments are being performed to operate an improved quantification by an enhancement of signal to noise ratio using a more homogeneous SNR between spectra acquired during stimulation and rest.

The values of metabolite concentrations reported here were in close agreement with those reported by Dienel et al. (2002) before, during and after 5 min of generalized sensory stimulation in the conscious rat: aspartate decreased by 0.7 µmol/g and glutamate increased by 0.8 µmol/g with respect to the rest period. These findings support an increased activity of the malate–aspartate shuttle (MAS) required for the maintenance of the cytosolic redox potential NADH/NAD + and ensuing glycolysis and synthesis of brain neurotransmitters (Lin et al., 2012). More importantly lactate increased by 1.1 µmol/g (+180%) in agreement with our +198% increase but in contrast with the recent human fMRS studies where lactate increases during stimulation were only between 10 and 30% (Mangia et al., 2007b; Lin et al., 2012). Quantification of Asp, Glu and Lac changes using LCModel fits to the sums of stimulation and rest spectra was in agreement with our findings relying on averages (Fig. 5). However, a 70% increase in lactate was found. This is in more agreement with the recent literature and our difference spectrum (Fig. 6E). We even hypothesize that this latter value may still be overestimated and confirm that an improved definition of the difference spectrum will definitively validate metabolic changes in the rat barrel cortex.

Elevated levels of brain lactate were reported in previous studies as discussed by Xu et al. (2005) who in contrast to us reported no significant changes in Lac in a rat model of sustained forepaw stimulation. However, a recent study by Wyss et al. (2011) also using electrical stimulation of the infraorbital branch of the trigeminal nerve with almost identical parameters of stimulation in rats demonstrated that Lac is indeed used at an increased rate by the brain to maintain neuronal activity. In addition, we also found an increase of lactate to a new steady state in agreement with studies by Mangia et al. in the human visual cortex.

Conclusion

In conclusion, the present results are comparable with previous fMRS studies in humans and support a rise in oxidative metabolism during brain activation. We hereby confirmed that sustained electrical trigeminal nerve stimulation represents a good model for investigating

the neurochemical consequences of barrel cortex activation during BOLD fMRI and fMRS studies and for characterizing the neurometabolic coupling in the rat barrel cortex (Lecrux et al., 2011). In addition, for the first time the dynamics of metabolite concentrations were evaluated during sustained somatosensory activation in the rat in vivo using ^{1}H fMRS.

Conflict of Interest

The authors have no conflict of interest to disclose.

Acknowledgments

This study was supported by the Centre d'Imagerie BioMédicale (CIBM) of Ecole Polytechnique Fédérale de Lausanne (EPFL), the University of Lausanne (UNIL) and the Foundations Leenards et Jeantet.

Appendix A. Supplementary data

Supplementary data to this article can be found online at http://dx.doi.org/10.1016/j.neuroimage.2013.02.042.

References

Bandettini, P.A., Kwong, K.K., Davis, T.L., Tootell, R.B., Wong, E.C., Fox, P.T., Belliveau, J.W., Weisskoff, R.M., Rosen, B.R., 1997. Characterization of cerebral blood oxygenation and flow changes during prolonged brain activation. Hum. Brain Mapp. 5 (2), 93–109.

Chen, W., Novotny, E.J., Zhu, X.H., Rothman, D.L., Shulman, R.G., 1993. Localized 1H NMR measurement of glucose consumption in the human brain during visual stimulation. Proc. Natl. Acad. Sci. U. S. A. 90 (21), 9896–9900.

Chung, S., Li, X., Nelson, S.B., 2002. Short-term depression at thalamocortical synapses contributes to rapid adaptation of cortical sensory responses in vivo. Neuron 34 (3), 437–446.

de Celis Alonso, B., Sergeyeva, M., Brune, K., Hess, A., 2012. Lateralization of responses to vibrissal stimulation: connectivity and information integration in the rat sensory-motor cortex assessed with fMRI. Neuroimage 62 (3), 2101–2109.

Dienel, G.A., Wang, R.Y., Cruz, N.F., 2002. Generalized sensory stimulation of conscious rats increases labeling of oxidative pathways of glucose metabolism when the brain glucose-oxygen uptake ratio rises. J. Cereb. Blood Flow Metab. 22 (12), 1490–1502.

Fanselow, E.E., Nicolelis, M.A., 1999. Behavioral modulation of tactile responses in the rat somatosensory system. J. Neurosci. 19 (17), 7603–7616.

Feldman, D.E., Brecht, M., 2005. Map plasticity in somatosensory cortex. Science 310 (5749), 810–815.

Friston, K.J., Frith, C.D., Turner, R., Frackowiak, R.S., 1995. Characterizing evoked hemodynamics with fMRI. Neuroimage 2 (2), 157–165.

Gruetter, R., Tkác, I., 2000. Field mapping without reference scan using asymmetric echo-planar techniques. Magn. Reson. Med. 43, 319–323.

Hyder, F., Chase, J.R., Behar, K.L., Mason, G.F., Siddeek, M., Rothman, D.L., Shulman, R.G., 1996. Increased tricarboxylic acid cycle flux in rat brain during forepaw stimulation detected with 1H[13C]NMR. Proc. Natl. Acad. Sci. U. S. A. 93 (15), 7612–7617.

Just, N., Petersen, C., Gruetter, R., 2010. BOLD responses to trigeminal nerve stimulation. Magn. Reson. Imaging 28 (8), 1143–1151.

Lecrux, C., Toussay, X., Kocharyan, A., Fernandes, P., Neupane, S., Lévesque, M., Plaisier, F., Shmuel, A., Cauli, B., Hamel, E., 2011. Pyramidal neurons are "neurogenic hubs" in the neurovascular coupling response to whisker stimulation. J. Neurosci. 31 (27), 9836–9847.

Lei, H., Mlynarik, V., Just, N., Gruetter, R., 2008. Snapshot gradient-recalled echo-planar images of rat brain at long echo time at 9.4 T. Magn. Reson. Imaging 26, 954–960.

Lin, Y., Stephenson, M.C., Xin, L., Napolitano, A., 2012. Morris PG investigating the metabolic changes due to visual stimulation using functional proton magnetic resonance spectroscopy at 7 T. J. Cereb. Blood Flow Metab. 32 (8), 1484–1495.

Lu, H., Mazaheri, Y., Zhang, R., Jesmanowicz, A., Hyde, J.S., 2003. Multishot partial k-space EPI for high-resolution fMRI demonstrated in a rat whisker barrel stimulation model at 3 T. Magn. Reson. Med. 50, 1215–1222.

Mangia, S., Tkác, I., Logothetis, N.K., Gruetter, R., Van de Moortele, P.F., Uğurbil, K., 2007a. Dynamics of lactate concentration and blood oxygen level-dependent effect in the human visual cortex during repeated identical stimuli. J. Neurosci. Res. 85 (15), 3340–3346.

Mangia, S., Tkác, I., Gruetter, R., Van de Moortele, P.F., Maraviglia, B., Uğurbil, K., 2007b. Sustained neuronal activation raises oxidative metabolism to a new steady-state level: evidence from 1H NMR spectroscopy in the human visual cortex. J. Cereb. Blood Flow Metab. 27 (5), 1055–1063.

Mangia, S., Giove, F., Tkác, I., Logothetis, N.K., Henry, P.G., Olman, C.A., Maraviglia, B., Di Salle, F., Uğurbil, K., 2009. Metabolic and hemodynamic events after changes in neuronal activity: current hypotheses, theoretical predictions and in vivo NMR experimental findings. J. Cereb. Blood Flow Metab. 29 (3), 441–463 (Mar).

Mlynárik, V., Gambarota, G., Frenkel, H., Gruetter, R., 2006. Localized short-echo-time proton MR spectroscopy with full signal-intensity acquisition. Magn. Reson. Med. 56 (5), 965–970.

Nielsen, A.N., Lauritzen, M., 2001. Coupling and uncoupling of activity-dependent increases of neuronal activity and blood flow in rat somatosensory cortex. J. Physiol. 533, 773–785.

Paxinos, G., Watson, C., 1998. The Rat Brain in Stereotaxic. Coordinates. Academic Press, San Diego.

Petersen, C.C.H., 2007. The functional organization of the barrel cortex. Neuron 56, 339–355.

Prichard, J., Rothman, D., Novotny, E., Petroff, O., Kuwabara, T., Avison, M., Howseman, A., Hanstock, C., Shulman, R., 1991. Lactate rise detected by 1H NMR in human visual cortex during physiologic stimulation. Proc. Natl. Acad. Sci. U. S. A. 88 (13), 5829–5831.

Provencher, S.W., 1993. Estimation of metabolite concentrations from localized in vivo proton NMR spectra. Magn. Reson. Med. 30 (6), 672–679 (Dec).

Quairiaux, C., Armstrong-James, M., Welker, E., 2007. Modified sensory processing in the barrel cortex of the adult mouse after chronic whisker stimulation. J. Neurophysiol. 97 (3), 2130–2147.

Strupp, J.P., 1996. Stimulate a GUI based fMRI analysis software package. Neuroimage 3, S607.

Uludağ, K., 2008. Transient and sustained BOLD responses to sustained visual stimulation. Magn. Reson. Imaging 26 (7), 863–869.

Woolsey, T.A., Van der Loos, H., 1970. The structural organization of layer IV in the somatosensory region (SI) of mouse cerebral cortex. The description of a cortical field composed of discrete cytoarchitectonic units. Brain Res. 17 (2), 205–242.

Wyss, M.T., Jolivet, R., Buck, A., Magistretti, P.J., Weber, B., 2011. In vivo evidence for lactate as a neuronal energy source. J. Neurosci. 31 (20), 7477–7485.

Xu, S., Yang, J., Li, C.Q., Zhu, W., Shen, J., 2005. Metabolic alterations in focally activated primary somatosensory cortex of alpha-chloralose-anesthetized rats measured by 1H MRS at 11.7 T. Neuroimage 28 (2), 401–409.

Yang, J., Shen, J., 2006. Increased oxygen consumption in the somatosensory cortex of alpha-chloralose anesthetized rats during forepaw stimulation determined using MRS at 11.7 Tesla. Neuroimage 32 (3), 1317–1325.

Yang, X., Hyder, F., Shulman, R.G., 1996. Activation of a single whisker barrel in rat brain localized by functional magnetic resonance imaging. Proc. Natl. Acad. Sci. U. S. A. 96, 475–478.

Yang, X., Hyder, F., Shulman, R.G., 1997. Functional MRI BOLD signal coincides with electrical activity in the rat whisker barrels. Magn. Reson. Med. 38, 874–877.